

# Reduction in photosystem II efficiency during a virus-controlled *Emiliana huxleyi* bloom

Susan A. Kimmance<sup>1,\*</sup>, Michael J. Allen<sup>1</sup>, António Pagarete<sup>1,2,3</sup>,  
Joaquín Martínez Martínez<sup>4</sup>, William H. Wilson<sup>1,4</sup>

<sup>1</sup>Plymouth Marine Laboratory, Prospect Place, The Hoe, Plymouth PL1 3DH, UK

<sup>2</sup>UPMC Univ. Paris 06, UMR 7144, Equipe Eppo: Evolution du Plancton et PaléoOcéans, Station Biologique de Roscoff, 29682 Roscoff, France

<sup>3</sup>Department of Biology, University of Bergen, Norway

<sup>4</sup>Bigelow Laboratory for Ocean Sciences, 60 Bigelow Drive, PO Box 380, East Boothbay, Maine 04544, USA

**ABSTRACT:** During viral infection of *Emiliana huxleyi*, laboratory studies have shown that photosystem (PS) II efficiency declines during the days post-infection and is thought to be associated with viral-induced interruption of electron transport rates between photosystems. However, measuring the impact of viral infection on PSII function in *E. huxleyi* populations from natural, taxonomically diverse phytoplankton communities is difficult, and whether this phenomenon occurs in nature is presently unknown. Here, chlorophyll fluorescence analysis was used to assess changes in PSII efficiency throughout an *E. huxleyi* bloom during a mesocosm experiment off the coast of Norway. Specifically, we aimed to determine whether a measurable suppression of the efficiency of PSII photochemistry could be observed due to viral infection of the natural *E. huxleyi* populations. During the major infection period prior to bloom collapse, there was a significant reduction in PSII efficiency with an average decrease in maximum PSII photochemical efficiency ( $F_v/F_m$ ) of 17% and a corresponding 75% increase in maximum PSII effective absorption cross-section ( $\sigma_{PSII}$ ); this was concurrent with a significant decrease in *E. huxleyi* growth rates and an increase in *E. huxleyi* virus (EhV) production. As *E. huxleyi* populations dominated the phytoplankton community and potentially contributed up to 100% of the chlorophyll *a* pool, we believe that the variable chlorophyll fluorescence signal measured during this period was derived predominantly from *E. huxleyi* and, thus, reflects changes occurring within *E. huxleyi* cells. This is the first demonstration of suppression of PSII photochemistry occurring during viral infection of natural coccolithophore populations.

**KEY WORDS:** Viral infection · *Emiliana huxleyi* bloom · Chlorophyll fluorescence · Photosystem II efficiency · Mesocosm

Resale or republication not permitted without written consent of the publisher

## INTRODUCTION

The bloom-forming *Emiliana huxleyi* (Lohmann) Hay and Mohler (Prymnesiophyceae) is the most abundant species of coccolithophore in the world's oceans and greatly impacts on marine ecosystems and, in particular, on global primary productivity

and biogeochemical cycling (Westbroek et al. 1993, Paasche 2001, Burkill et al. 2002). It is now widely accepted that viruses (from the genus *Coccolithoviruses*) are intrinsically linked to the demise of *E. huxleyi* populations (Bratbak et al. 1993, Jacquet et al. 2002, Wilson et al. 2002, Schroeder et al. 2003) and, via the 'kill the winner' strategy (Thingstad &

\*Corresponding author: sukim@pml.ac.uk

Lignell 2007), play a key role in controlling blooms. Viral infection of a phytoplankton cell inevitably results in physiological consequences to the host metabolism, leading to the activation of stress and defence mechanisms (Bidle et al. 2007, Vardi et al. 2009), which in turn can alter growth dynamics and lifecycle (Frada et al. 2008). One such consequence is a viral-induced disruption of photosynthesis, thought to be associated with a reduced efficiency of electron capture by photosystem (PS) II reaction centres from the light-harvesting pigments (Seaton et al. 1995, Juneau et al. 2003) and inhibition of electron transport between PSII and PSI (Teklemariam et al. 1990, Seaton et al. 1995, Balachandran et al. 1997), potentially leading to elevated oxidative stress within cells as a result of uncontrolled singlet oxygen production (Asada 1994, Evans et al. 2006). Changes in photosynthetic activity can have major implications for the physiological status of autotrophic cells, which, in turn, will have ecological and biogeochemical consequences. Several studies have investigated the changes in phytoplankton photosynthesis during viral infection (e.g. Waters & Chan 1982, Van Etten et al. 1983, Teklemariam et al. 1990, Suttle 1992, Suttle & Chan 1993, Juneau et al. 2003) and most, but not all (Hewson et al. 2001, Lindell et al. 2005), have shown reduced photosynthetic activity at some point following viral enrichment. During infection of *Micromonas pusilla*, though photosynthesis declined only at the point of lysis, photosystems (particularly PSII complexes) were functioning with a higher biochemical turnover rate during late infection and lysis (Brown et al. 2007). This increased demand on PSII during infection may impact on rates of carbon fixation even before cell lysis, which could have major implications for oceanic primary productivity if this mechanism is common in other phytoplankton species. However, measuring the impact of viral infection on PSII efficiency in natural phytoplankton populations is difficult, particularly when other environmental factors such as nutrient availability or taxonomic shifts (see Suggett et al. 2009 for review) can confound the results. Consequently, despite several studies investigating the viral-induced decline of natural *E. huxleyi* blooms (e.g. Bratbak et al. 1993, Egge & Heimdahl 1994, Jacquet et al. 2002, Martínez Martínez et al. 2007, Pagarete et al. 2009), to date, there are no studies attempting to examine the photophysiological stress-response of natural *E. huxleyi* populations during viral infection.

Recently, changes in photophysiology using chlorophyll *a* (chl *a*) fluorescence measurements have become an important and easily measurable param-

eter of the physiological state of phytoplankton such as *Emiliania huxleyi* (Suggett et al. 2009). Variations in parameters such as the maximum PSII photochemical efficiency ( $F_v/F_m$ ) and the maximum PSII effective absorption cross-section ( $\sigma_{\text{PSII}}$ ) are frequently used as indicators of physiological state in phytoplankton (Geider & La Roche 1994, Timmermans et al. 2001, Moore et al. 2006). Environmental factors such as nutrient limitation or light stress have been shown to produce a distinct change in  $F_v/F_m$  detectable using chl *a* fluorescence analysis of PSII photochemistry (see Suggett et al. 2009 for a review). Viral infection has also been shown to decrease  $F_v/F_m$  (Seaton et al. 1995, Hewson et al. 2001, Juneau et al. 2003), and previous laboratory studies have shown that during viral infection of *E. huxleyi* there is generally a trend towards a decreased  $F_v/F_m$  during the days post-infection as the cultures lyse (Evans et al. 2006, Bidle et al. 2007, Llewellyn et al. 2007). However, this phenomenon has never been examined during a natural *E. huxleyi* bloom scenario. As measurements of the efficiency of PSII have proved to be a reliable indicator of infection stress during laboratory *E. huxleyi* experiments, the physiological stress caused by viral infection in natural populations might also be measurable using chl *a* fluorescence analysis of PSII photochemistry.

Given the importance of viral reduction of global primary production in terms of carbon flux and biogeochemical cycling (Suttle 2007), we examined the temporal changes in PSII photochemistry during the infection period of an *Emiliania huxleyi* bloom. To test the hypothesis that viral infection suppresses PSII photochemistry in natural *E. huxleyi* populations, causing a decrease in  $F_v/F_m$ , we took advantage of a field mesocosm experiment that was conducted at the large-scale facilities at the Marine Biological Field Station, University of Bergen, Norway in June 2008. During the mesocosm experiment, large volume ( $>10 \text{ m}^3$ ) enclosures were nutrient-manipulated to induce *E. huxleyi* blooms under phosphate-replete conditions to investigate the role of phosphorus (P)-availability on coccolithovirus–*E. huxleyi* dynamics (Pagarete et al. 2009).

## MATERIALS AND METHODS

### Study site and experimental design

The mesocosm experiment was carried out in Raunefjorden, western Norway, at the Marine Biological Field Station in Espeland, 20 km south of Bergen,

from 2 until 25 June 2008. Three enclosures of 11 m<sup>3</sup> (4 m deep and 2 m wide) made of 0.15 mm thick polyethylene (90% light penetration of the photosynthetic active radiation) were mounted on floating frames moored along the south side of a raft in the middle of the bay (for details see Egge & Aksnes 1992) and numbered 1 to 3 in an east–west direction. The enclosures were filled simultaneously on 3 June with unfiltered, unscreened seawater from 2 m depth using a submersible centrifugal pump. The seawater in the enclosures was kept homogeneous by means of airlifts (gentle water mixers). To induce a bloom of *Emiliania huxleyi*, nutrients were added daily as concentrated stock solutions (between 13:00 and 14:00 h; after the daily sampling) in a nitrogen:phosphorus (N:P) ratio of 15:1 (1.5  $\mu\text{mol l}^{-1}$  NaNO<sub>3</sub> and 0.1  $\mu\text{mol l}^{-1}$  KH<sub>2</sub>PO<sub>4</sub>) from 4 to 21 June 2008. Nutrient concentrations were analysed once daily using standard methods (Strickland & Parsons 1968) adapted to an auto-analyzer equipped with autosampling, detection and computing methods from SANplus segmented Flow Analyzer (Skalar Analytic). Briefly, a 100 ml sample was taken daily from each enclosure, preserved in chloroform (0.8% final concentration) and stored in the dark at 4°C prior to analysis.

### Phytoplankton abundance and composition

Phytoplankton composition and abundance estimates were determined 4 times daily (06:00, 12:00, 18:00 and 00:00 h) from all enclosures and directly from Raunefjorden surface waters by analysis of fresh samples on a FACScan flow cytometer (Becton Dickinson) equipped with a 15 mW laser exciting at 488 nm and with a standard filter set up. Samples were analysed at high flow rate ( $\sim 70 \mu\text{l min}^{-1}$ ) and specific phytoplankton groups were discriminated by differences in their forward or right angle light scatter (FALS, RALS) and chl *a* (and phycoerythrin for *Synechococcus* populations) fluorescence. Files were analysed using WinMDI 2.8 software (J. Trotter, <http://facs.scripps.edu>). Flow cytometric analysis (FCM) allowed us to identify the major microbial groups that developed and to examine in fine detail the temporal changes in microbial dynamics that occurred during this experiment. Based on the flow cytometric profiles (Jacquet et al. 2002) and verified by molecular analysis (Pagarete et al. 2009, Sorensen et al. 2009), the coccolithophore populations and large, virus-like particles (LVLP), were identified as *Emiliania huxleyi* and *E. huxleyi* virus (EhV) genotypes respectively.

### Virus abundance

Virus abundance was determined 4 times daily (see previous section) using the flow cytometric protocol of Brussaard (2004). Samples for viral analysis were fixed with glutaraldehyde (0.5% final concentration) for 30 min at 4°C, snap frozen in liquid N and stored at  $-80^{\circ}\text{C}$ . Samples were subsequently defrosted at room temperature and diluted 500 fold with TE buffer (10 mmol l<sup>-1</sup> Tris-HCL pH8, 1 mmol l<sup>-1</sup> EDTA), stained with SYBR Green 1 (Molecular Probes; Marie et al. 1999) at a final dilution of  $5 \times 10^{-5}$  the commercial stock, incubated at 80°C for 10 min in the dark, then allowed to cool for 5 min before analysis using a FACSort flow cytometer (Becton Dickinson). Samples were analysed for 2 min at a flow rate of  $\sim 70 \mu\text{l min}^{-1}$ , and virus groups were discriminated on the basis of their RALS versus green fluorescence. Data files were analysed using WinMDI 2.8 software (see previous section).

### Chlorophyll fluorescence measurements using FIRE fluorometry

To assess phytoplankton PSII quantum efficiency during the experiment, discrete variable-chlorophyll fluorescence measurements were acquired 3 times daily (12:00, 18:00 and 00:00 h) using a fluorescence induction and relaxation (FIRE) fluorometer (Satlantic). Prior to each fluorescence measurement, samples were dark-adapted for 15 to 20 min at a controlled temperature to match *in situ* conditions. Dark-adapted samples (3 ml) and 0.2  $\mu\text{m}$  filtered sample controls (blanks) were analysed within cylindrical 1-cm path-length cuvettes placed into the FIRE fluorometer cuvette holder. Excitation was provided by a high luminosity (up to 1 W/cm<sup>2</sup>) blue and green LED array (450 and 500 nm peak heights, each with 30 nm bandwidth). Filtered (0.2  $\mu\text{m}$ ) sample controls (blanks) were analysed at the gain chosen for the measurement on the sample and subtracted from the sample fluorescence sequence at the time of fitting the Kolber-Prasil-Falkowski model (KPF, Kolber et al. 1998). Cell-free controls showed no soluble fluorescence (*sensu* Cullen & Davis 2003). The retrieved PSII photochemistry parameters utilized in this study are the minimum fluorescence ( $F_0$ ; the initial fluorescence emitted when all the reaction centres are open) and the maximum fluorescence ( $F_m$ ; maximal fluorescence corresponding to all the reaction centres being closed) yields, the maximum photochemical efficiency of PSII ( $F_v/F_m$ ) and the relative functional absorption

cross-section of PSII,  $\sigma_{\text{PSII}}$  (the product of the light-harvesting capability of the light-harvesting pigments and the efficiency of excitation transfer to the reaction centre) (Kolber & Falkowski 1993).

### Chlorophyll analysis

Samples for chl *a* analysis (Parsons et al. 1984) were filtered at 5 mm Hg onto GF/F glass fibre filters, which were then wrapped in aluminium foil and snap frozen in liquid N. Triplicate samples were stored at  $-20^{\circ}\text{C}$  in darkness until they could be analysed. Filters were then extracted in cold 90% acetone in darkness for 24 h prior to analysis on a Turner Design Model 10-AU fluorometer.

## RESULTS

### Mesocosm phases and composition

Daily additions of N and P to the enclosed fjord water within the mesocosms stimulated phytoplankton growth. Throughout the experiment, 4 major groups were discernible at varying concentrations using flow cytometry: *Synechococcus* spp., picoeukaryotes, nanoeukaryotes and *Emiliana huxleyi* (Fig. 1). Temporal progression and succession of the phytoplankton community appeared to be split into 3 distinct phases over the 17 d study (Fig. 2): Phase 1 was between Days 1 to 7 and was dominated by *Synechococcus* spp., nanoeukaryotes and, to a lesser degree, picoeukaryotes; Phase 2 (Days 7 to 13) was primarily characterized by exponential growth and dominance of the *E. huxleyi* populations; and during Phase 3 (Days 13 to 17) collapse of the *E. huxleyi* populations occurred, with a concurrent exponential increase in EhV concentrations (Figs. 2 & 3). Phytoplankton community shifts were also reflected in temporal changes in nutrient concentrations during the experiment (Fig. 4), with 3 phases of drawdown of nutrients: after Day 3, corresponding to the increase in the nanoeukaryote populations; after Day 9, corresponding with the initiation of the *E. huxleyi* blooms and after Day 15, which was probably a result of the post-bloom succession of the other phytoplankton groups. During the 17 d experiment, phos-

phate concentrations ranged from 0 to  $0.28 \mu\text{mol l}^{-1}$  (Fig. 4A) and nitrate concentrations fluctuated but remained consistently low,  $<2.5 \mu\text{mol l}^{-1}$ , with a marked decline after Day 9 to beyond the limit of detection (Fig. 4B); this was followed by an observed increase to  $1 \mu\text{mol l}^{-1}$  in the final phase of the exper-

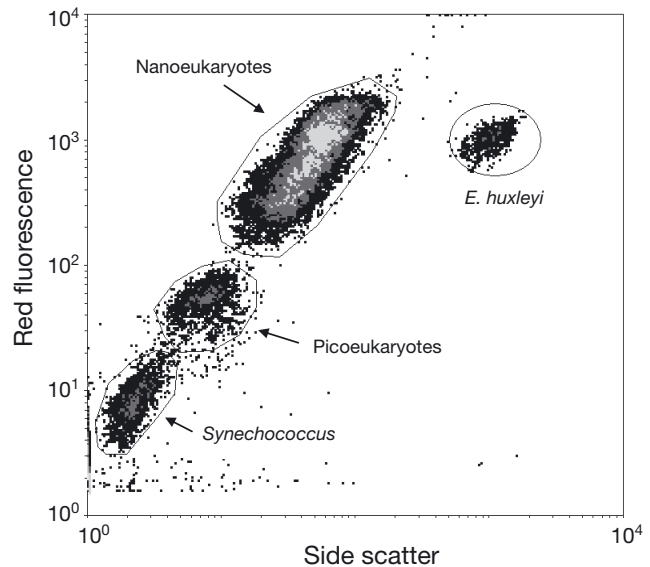


Fig. 1. Typical flow cytometry scatter plot distinguishing the 4 groups identified in the photosynthetic community (*Emiliana huxleyi*; nanoeukaryotes; picoeukaryotes and *Synechococcus*). Populations were discriminated based on their differences in side scatter and chl *a* red fluorescence (FL3), and phycoerythrin for *Synechococcus* populations (FL2)

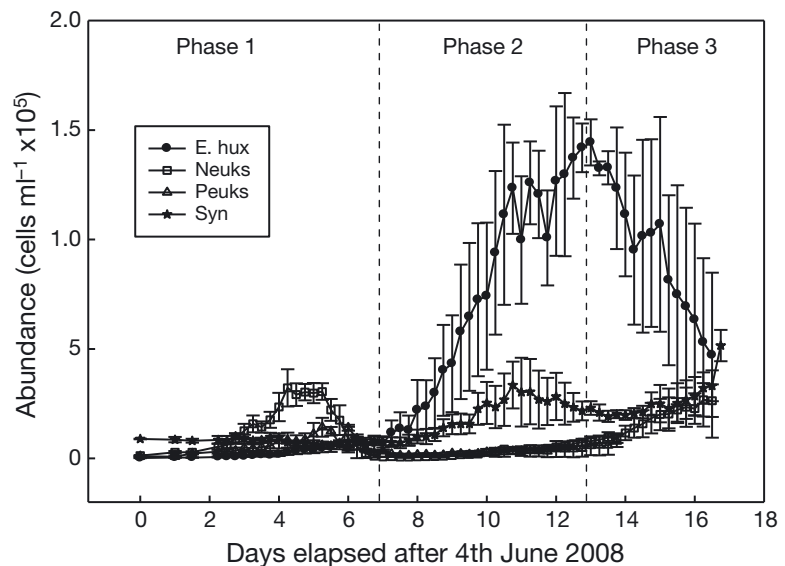


Fig. 2. Development of the phytoplankton community: (E.hux) *Emiliana huxleyi*; (Peuks) picoeukaryotes; (Neuks) nanoeukaryotes; (Syn) *Synechococcus* spp. measured 4 times per day in all mesocosms during the 3 phases of the experiment. Symbols are the mean values of the triplicate mesocosms; error bars represent 1 SD

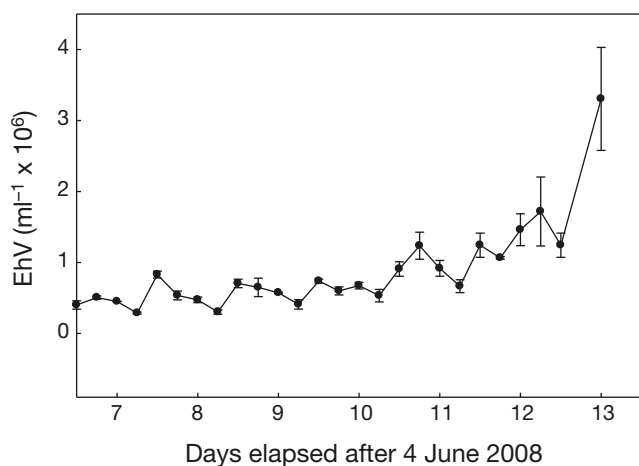


Fig. 3. EhV concentrations during Phase 2 of the experiment (viral particles  $\text{ml}^{-1}$ ) measured using flow cytometry. Symbols are the mean values of the triplicate mesocosms; error bars represent 1 SD

iment. N:P ratios largely reflected the N concentrations in each of the treatments since P concentrations were low (Fig. 4C).

*Emiliana huxleyi* increased exponentially from Day 7 onwards (Fig. 2), and average *E. huxleyi* specific net growth rates during the first part of Phase 2 (Days 7 to 10) were  $0.71 \pm 0.1 \text{ d}^{-1}$  (mean  $\pm$  SD). Daily net growth rates of *E. huxleyi* ( $\mu \text{ d}^{-1}$ ) were calculated as:  $\ln(N_t/N_0)/t$ , where  $N_t$  and  $N_0$  are the final and initial measured *E. huxleyi* abundances respectively, and  $t$  is 24 h. In contrast, both picoeukaryote and nanoflagellate populations exhibited slow and variable increases in abundance during this period and cell biomass was extremely low compared to the *Synechococcus* and *E. huxleyi* populations (Fig. 2). *E. huxleyi* made up an average of  $75 \pm 5\%$  of the phytoplankton community in terms of cell abundance during Days 7 to 13, compared to only  $19 \pm 5\%$ , and  $3 \pm 1\%$  for the *Synechococcus* and nanoeukaryote and picoeukaryote populations, respectively. Although *Synechococcus* concentrations represented up to 19% of the phytoplankton biomass, a maximum was reached by Day 10 (Fig. 2); whereas *E. huxleyi* cell concentrations continued to increase until Day 13, reaching a maximum of  $1.7 \times 10^5 \text{ ml}^{-1}$ . Concurrently, EhV concentrations increased exponentially from a low of  $2 \times 10^5 \text{ ml}^{-1}$  at the start of Phase 2 to concentrations of  $\sim 1 \times 10^7 \text{ ml}^{-1}$  by Day 13 (Fig. 3). Daily *in situ* chl *a* concentrations followed a similar pattern to phytoplankton abundance, with 2 peaks in biomass during the experiment: on Days 5 and 10, chl *a* increased to maximum average concentrations of  $5.7 \pm 0.9 \mu\text{g ml}^{-1}$  and  $15.73 \pm 4.3 \mu\text{g ml}^{-1}$  respectively, across all mesocosms (Fig. 5).

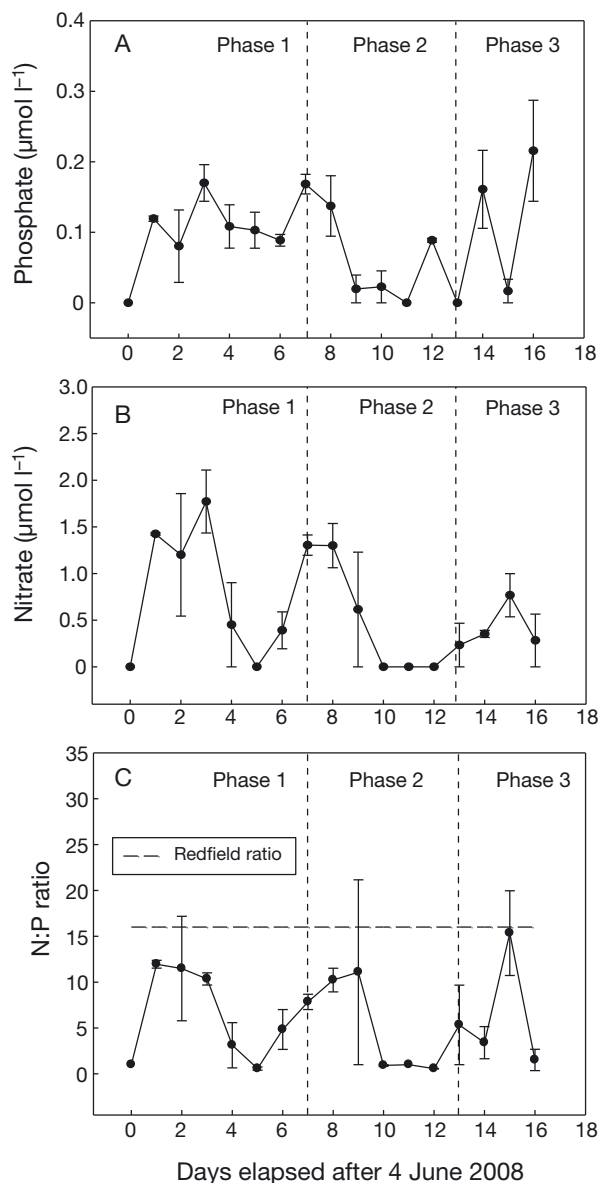


Fig. 4. Dynamics of (A)  $\text{PO}_4$  and (B)  $\text{NO}_3$  concentrations measured once daily in the mesocosms ( $1.5 \mu\text{mol l}^{-1} \text{ NaNO}_3$  and  $0.1 \mu\text{M KH}_2\text{PO}_4$ ) during the experiment. (C) Progression of the ratio between N and P. The dashed line symbolizes the Redfield ratio (the theoretical optimum N:P ratio for near maximal phytoplankton growth). Symbols are the mean values of the triplicate mesocosms; error bars represent 1 SD

#### Temporal changes in chlorophyll fluorescence and photosystem II efficiency

As the decline in *Emiliana huxleyi* was so dramatic during Phase 3 and, thus, populations would contain a high proportion of lysing cells which could potentially interfere with the variable chlorophyll fluorescence signal, we present the temporal changes in



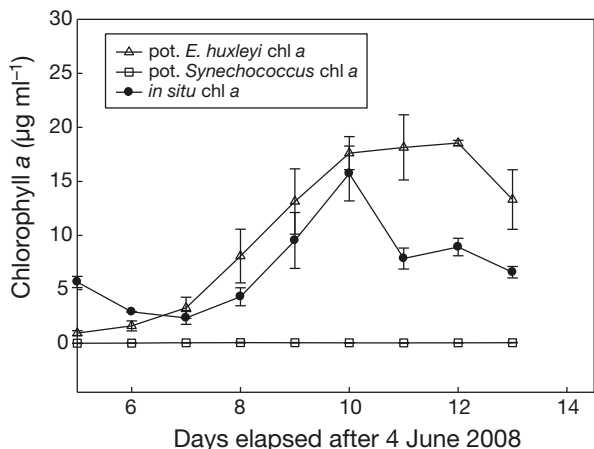


Fig. 5. Temporal changes in chl *a* concentrations ( $\mu\text{g ml}^{-1}$ ) during Phase 2 of the experiment. Symbols represent the mean values of the triplicate mesocosms; error bars represent 1 SD. Estimated potential (pot.) contributions of *Emiliana huxleyi* ( $\Delta$ ) and *Synechococcus* populations ( $\square$ ) to the total *in situ* chl *a* pool ( $\bullet$ ) based on an assumed cell-specific chlorophyll content (see 'Temporal changes in chlorophyll fluorescence and photosystem II efficiency' for details)

PSII efficiency only between Days 7 and 13, which was the main period of *E. huxleyi* infection prior to bloom collapse, based on major capsid protein (MCP) expression data (Pagarete et al. 2009). In addition, as our aim was to investigate changes in PSII efficiency of *E. huxleyi* cells, and the variable chlorophyll fluorescence measurements were taken from natural samples with a potentially mixed assemblage of phytoplankton, we estimated how much of the variable chlorophyll fluorescence signal potentially came from *E. huxleyi*. Based on an estimated cell-specific chl *a* content of  $0.14 \text{ pg cell}^{-1}$  for *E. huxleyi* (average of literature values 0.06 to 0.29; Fritz & Balch 1996, Muggli & Harrison 1996, Pond & Harris 1996, Wolfe & Steinke 1996, Llewellyn et al. 2007), we calculated that the *E. huxleyi* populations potentially contributed between 70 and 100% towards the total chl *a* pool during this period (average of 3 mesocosms, Fig. 5). In contrast, *Synechococcus* spp. (the second most abundant phytoplankton group measured during this time) may have contributed only 0.5 to 1.2% to total chl *a* (based on an estimated cell-specific chl *a* content of 0.003 pg; Morel et al. 1993). Thus, we believe that the variable chlorophyll fluorescence signal measured during Phase 2 and the start of Phase 3 (Days 7 to 13) was derived predominantly from *E. huxleyi* and, thus, reflects changes occurring within *E. huxleyi* cells.

As *Emiliana huxleyi* biomass increased rapidly and became dominant after Day 7, a diel pattern in

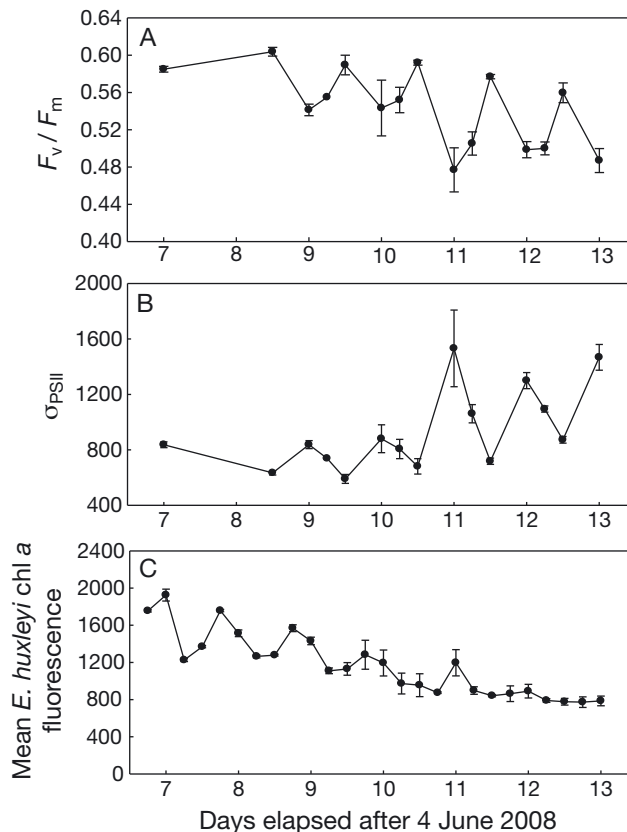


Fig. 6. Changes in photosynthetic community fluorescence parameters during Phase 2 of the experiment: (A)  $F_v/F_m$ ; (B)  $\sigma_{\text{PSII}}$ ; and (C) mean *Emiliana huxleyi* chlorophyll fluorescence per cell (arbitrary units; derived using flow cytometry). Symbols are the mean values of the triplicate mesocosms; error bars represent 1 SE. All parameters were measured 3 times per day in all mesocosms

PSII efficiency became clear (Fig. 6A,B), with the lowest  $F_v/F_m$  and highest  $\sigma_{\text{PSII}}$  values recorded at midday, corresponding to the daily light cycle. Day length during the experiment was 18 h on average, typically with sunrise at 05:00 h and sunset at 23:00 h. Between Days 7 and 13, there was a significant decrease in  $F_v/F_m$  ( $p < 0.01$ ), across all mesocosms and sampling times (midday, 18:00 h and midnight) with an average decline of  $11.76 \pm 5.86\%$  (mean  $\pm$  SD) and a maximum of 14.6%. Across all mesocosms, the midday measurements showed the greatest temporal decrease in PSII efficiency, and the average decline in  $F_v/F_m$  at this time point between Days 7 and 13 was  $16.8 \pm 3.37\%$ . The largest decrease in  $F_v/F_m$  was observed between Days 10 and 11 and corresponded with the timing of a significant increase in MCP expression (Pagarete et al. 2009);  $F_v/F_m$  decreased by 21% during this time. In fact, when the relationship between temporal changes in MCP

expression and  $F_v/F_m$  was compared during Days 7 to 13, we found that they were significantly related at the 0.01 level.

In contrast to  $F_v/F_m$ ,  $\sigma_{\text{PSII}}$  increased significantly ( $p < 0.01$ ) between Days 7 and 13: the average increase across all mesocosms and times was  $45.97 \pm 25.91\%$ . However, similarly to  $F_v/F_m$ , the largest increases in  $\sigma_{\text{PSII}}$  occurred between the daily midday measurements, where maximum increases in  $\sigma_{\text{PSII}}$  of  $75.4 \pm 17.23\%$  were observed. In addition, comparable to  $F_v/F_m$ , the increase in  $\sigma_{\text{PSII}}$  was greatest between Days 10 and 11, with a maximum increase of 114% during this time.

As *Emiliania huxleyi* biomass increased between Days 7 and 13, the timing of changes to  $F_v/F_m$  and  $\sigma_{\text{PSII}}$  also corresponded with a simultaneous significant decrease in mean chl *a* fluorescence per *E. huxleyi* cell (obtained from flow cytometric analysis;  $p < 0.001$ , Fig. 6C). The average decrease was  $54.19 \pm 6.34\%$ , with no significant difference between time points or mesocosms. Mean chl *a* fluorescence per *E. huxleyi* cell generally followed a diel trend, with maximal values typically at dusk (Fig. 6C), as previously found by Jacquet et al. (2002). The largest decline in chl *a* fluorescence per cell occurred between Days 11 and 12 across all mesocosms and time points, corresponding with the significant increase in MCP expression (Pagarete et al. 2009). As *E. huxleyi* was the dominant phytoplankton during Days 7 to 13, and chl *a* fluorescence levels had almost halved in these cells by Day 13, this decrease may explain why *in situ* bulk chl *a* levels decreased sharply after Day 10 to  $6.6 \pm 0.91 \mu\text{g ml}^{-1}$  on Day 13 (Fig. 5) despite *E. huxleyi* populations increasing until Day 13 (Fig. 2).

## DISCUSSION

Addition of nutrients to fjord seawater enclosures stimulated microbial succession and induced *Emiliania huxleyi* blooms, which subsequently collapsed with corresponding increases in virus particles (EhV). Based on the rapid increase in EhV corresponding with the decline in *E. huxleyi* and estimates of viral-induced mortality that were up to 100% of total *E. huxleyi* mortality (Vardi et al. 2012), we assume that viruses caused the major collapse of the *E. huxleyi* populations. This view is further supported by previous experimental data from studies that induced near monospecific blooms of *E. huxleyi* under similar conditions (Bratbak et al. 1993, Egge & Heimdahl 1994, Castberg et al. 2001, Jacquet et al. 2002, Schroeder et al. 2003, Martínez Martínez et al. 2007).

Although results from this experiment are comparable with those of previous studies, this is the first to report changes in the efficiency of PSII photochemistry during viral-induced bloom decline of a natural, *E. huxleyi*-dominated phytoplankton community. Collapse of the *E. huxleyi* populations was rapid, as found previously (Bratbak et al. 1993, Castberg et al. 2001, Jacquet et al. 2002). Prior to bloom collapse, there was a significant suppression of PSII photochemical efficiency which occurred concurrently with increased EhV abundance and a decline in *E. huxleyi* growth rates, as observed in laboratory studies with *E. huxleyi* and EhV (Evans et al. 2006, Bidle et al. 2007, Llewellyn et al. 2007). This correlation in timing between the depression of PSII efficiency and viral-induced collapse of *E. huxleyi* suggests that these 2 factors may indeed be linked and, moreover, that viral stress may be instrumental in the decline of *E. huxleyi* photophysiology in natural populations. To our knowledge, this is the first study that attempts to bridge what is observed in the laboratory with what is observed in nature.

Although here we cannot derive a direct mechanistic link between the viral-induced demise of *Emiliania huxleyi* and the observed changes in PSII photochemistry, previous laboratory studies of both plant and algal virus systems have clearly demonstrated a significant inhibition of photosynthesis during infection (e.g. Waters & Chan 1982, Suttle et al. 1990, Balachandran et al. 1997, Juneau et al. 2003) and have revealed mechanisms that may also be applicable to natural coccolithophore populations. Typically, inhibition of photosynthesis occurs as a result of indirect viral interference with electron flow, thought to be associated with the change from host protein and nucleic acid synthesis to synthesis of virus-encoded protein and nucleic acid (Teklemariam et al. 1990, Seaton et al. 1995). Subsequently, there is a loss of PSII-PSI electron transport efficiency due to destabilisation of PSII-dependent protein turnover (Van Etten et al. 1991), observed as a reduction in photochemical quenching and an increase in fluorescence quenching, and indicated by a decrease in dark-adapted  $F_v/F_m$  (Teklemariam et al. 1990, Seaton et al. 1995, Seaton et al. 1996, Balachandran et al. 1997, Rahoutei et al. 2000, Hewson et al. 2001, Juneau et al. 2003). Furthermore, oxidative stress is elevated within infected cells (Schwarz 1996, Evans et al. 2006, Bidle et al. 2007, Vardi et al. 2009), and the production of reactive oxygen species (ROS) through viral-induced destabilisation of PSII turnover has been suggested as a causal factor (Balachandran et al. 1997, Evans et al. 2006). Here, we cannot demon-

strate that the changes in PSII function were directly linked to viral infection, only that the efficiency of PSII photochemistry appeared to be reduced during the infection period of the *E. huxleyi* bloom, concurrent with an exponential increase in EhV. However, supporting results from this same mesocosm study do show increased production of intra- and extra-cellular ROS within *E. huxleyi* cells during the infection and lysis period (Vardi et al. 2012). Thus, with the additional recent discovery that virus-induced *E. huxleyi* cell death appears to be crucially mediated by viral sphingolipid-induced ROS production (Bidle & Vardi 2011, Vardi et al. 2012), it is tempting to speculate that the decreased  $F_v/F_m$  observed here may have been a result of increased ROS generation produced during viral infection and replication.

### The potential influence of other environmental factors

Of course, other environmental stressors can also impact PSII photochemistry (Suggett et al. 2009). Thus, as this experiment was conducted with natural populations in a changeable environment, it could be argued that an alternative explanation for the changes in  $F_v/F_m$  and  $\sigma_{\text{PSII}}$  observed here is that of environmental variations in nutrient status or light intensity (Kolber et al. 1988, Geider et al. 1993, Graziano et al. 1996, Moore et al. 2008, Ragni et al. 2008) or a shift in the taxonomic community composition (Moore et al. 2006, Suggett et al. 2009) rather than viral infection. However, we consider that these additional factors were not the significant contributors to the observed changes in photosystem II efficiency, and here we briefly present our reasoning.

This study is not without its limitations in that attempting to extract specific information about the photophysiological status of *Emiliania huxleyi* from natural, mixed populations has a degree of error because of the taxonomic signal from the other phytoplankton groups (Suggett et al. 2009). However, unlike most natural phytoplankton communities, which contain a diverse mixture of photosynthetic algal groups, establishment of a dominant *E. huxleyi* bloom means that the majority of the fluorescence signal obtained from the analysis is most likely derived from these populations. Within a natural phytoplankton community, the algal group that contributes the greatest proportion of the total chl *a* fluorescence dominates the mixed community value measured for  $F_v/F_m$  and  $\sigma_{\text{PSII}}$  (Suggett et al. 2004). Based on the current experimental design, we cannot

say that *E. huxleyi* were the sole contributors to the fluorescence signal. However, by combining phytoplankton community analysis via flow cytometry with estimates of cell-specific chlorophyll content, we were able to show that at least during the peak of the blooms, *E. huxleyi* populations not only dominated, but also had the potential to produce the majority of the chl *a* fluorescence signal (up to 100% at the peak of the bloom). Future field studies, however, could remove any uncertainty by including additional measurements of size-fractionated diagnostic marker pigments, and conducting flow cytometric cell sorting of specific phytoplankton populations (Zubkov & Tarran 2008) for single-cell chlorophyll fluorescence analysis (Gachon et al. 2006) of infected versus non-infected cells (Martínez Martínez et al. 2011).

The utility of using changes in the maximum quantum yield of PSII ( $F_v/F_m$ ) as an indicator of nutrient stress in phytoplankton is a contentious issue (Cullen et al. 1992, Parkhill et al. 2001, Kruskopf & Flynn 2006), with contrasting results reported (e.g. Graziano et al. 1996, Moore et al. 2006, Sylvan et al. 2007). While Kolber et al. (1988) found a significant reduction in the photosynthetic efficiency of PSII under N limitation, Kruskopf & Flynn (2006) showed no consistent trends in  $F_v/F_m$  with which to gauge nutrient status in N and P-limited phytoplankton cultures. In this study, we aimed to ensure that the mesocosms were in a nutrient-replete status throughout the experiment and, therefore remove any potential influence of nutrient limitation on PSII efficiency. Thus, the daily nutrient addition (up to Day 16) suggested that nutrients (at least N and P) should not have been limiting in these mesocosms and, compared to other factors, PSII function should have been insensitive to small fluctuations in the N:P supply ratio. Although N:P ratios were less than the classically optimal Redfield N:P ratio of 16:1 throughout most of the experiment, conditions of high mortality, such as during intense grazing or in this case high viral infection, can lead to a lowered optimal N:P ratio (Klausmeier et al. 2004). Moreover, Geider & La Roche (2002) showed that the critical N:P ratio of natural marine phytoplankton is typically much lower than 16, and can be less than 5 during phytoplankton blooms. During the peak of the *Emiliania huxleyi* bloom (Days 10 to 14), N:P ratios in the mesocosms dipped below 5, suggesting possible N-limitation at this point. However, the competitive ability of *E. huxleyi* to use regenerated N and exploit nutrient-limited conditions (Lessard et al. 2005) suggests that their growth at least was not limited by the N and P ratios available. Further evidence supporting this is



their high abundance during bloom increase (max.  $\mu = 0.93 \text{ d}^{-1}$ ), with corresponding  $F_v/F_m$  of 0.6, suggesting cells were growing at their maximum. Furthermore, as estimates of viral-induced mortality rates were up to 100% (see above), the demise of the *E. huxleyi* populations was assumed to be virus-driven rather than through exhaustion of nutrients.

In addition to nutrients, light availability is one of the most important controlling factors for phytoplankton growth, and in the natural environment phytoplankton typically display a diel photosynthetic pattern stimulated by the daily light cycle and an inbuilt circadian rhythm (Falkowski & Raven 2007). Changes in *Emiliania huxleyi* photophysiology were clearly linked to the daily light cycle and, over the 24 h period, lowest  $F_v/F_m$  values and highest  $\sigma_{\text{PSII}}$  measurements were obtained at midday, as has been found previously for natural, coastal phytoplankton communities (Vassiliev et al. 1994). However, unlike the diurnal suppression of PSII efficiency which typically completely recovers during the dark, here we observed a sustained reduction in PSII efficiency between Days 7 and 13, with no daily recovery. It is possible that day-to-day variability in light during this phase of the experiment may have influenced this decrease in *E. huxleyi* photochemistry, as increasing light stress typically causes a depression in PSII efficiency (Vassiliev et al. 1994, Baker 2008). Unfortunately, daily irradiance measurements were not available during this study so we cannot rule out the light-driven suppression of PSII photochemistry between Days 7 to 13 completely. However, when we compared day-to-day changes in light simply in terms of overcast versus clear days, there was no clear evidence that light was driving the reduction in PSII efficiency. This is in agreement with the results of Ragni et al. (2008) who showed the insensitivity of *E. huxleyi* to light-induced photoinhibition because of efficient photorepair mechanisms, and suggests an alternative causal factor.

### Biogeochemical implications

Although a reduction in PSII capacity is not necessarily an indication of reduced carbon acquisition due to compensatory mechanisms (Behrenfeld 1998, Falkowski & Raven 2007), increased energetic costs for the phytoplankton host during infection due to monopolization of the cytoplasmic carbon and/or phosphate pools for viral replication (Seaton et al. 1995) has previously been shown to reduce carbon dioxide ( $\text{CO}_2$ ) fixation and potentially growth (Suttle

1992). For a globally important photosynthetic eukaryote such as *E. huxleyi*, this potential alteration of carbon fixation rates pre-lysis could have significant implications for global oceanic primary production and the biological carbon pump (Volk & Hoffert 1985). As a rough estimate of what this impact could be, applying our results to the linear model of Smyth et al. (2004) (which predicts primary productivity from biophysical parameters), we find that the observed decrease in  $F_v/F_m$  during the bloom period of our experiment (Days 7 to 13) could potentially translate to a 17% reduction in *Emiliania huxleyi* primary production. This would be a significant loss of carbon from the marine microbial food web which would not be included in calculations that were based on changes in cell abundance measurements alone. As the potential changes in carbon fixation occur pre-lysis, this could have crucial implications for the efficiency of carbon transfer to higher trophic levels. This is an additional loss of photosynthetically fixed carbon that is currently not accounted for in the 'viral shunt': the assumption that viruses divert between 6 and 26% to the dissolved organic matter pool (Wilhelm & Suttle 1999). Therefore, future studies should include more detailed assessments of host photophysiology at a cellular level, and determine rates of both  $\text{O}_2$  evolution and  $\text{CO}_2$  fixation throughout the entire virus lytic cycle to fully assess the implications for host photosynthesis and nutrient and energy flux.

### CONCLUSIONS

Previously, there has been contention regarding the use of  $F_v/F_m$  as an indicator of stress (e.g. Parkhill et al. 2001, Young & Beardall 2003, Kruskopf & Flynn 2006) or physiological change (Baker 2008, Moore et al. 2008, Suggett et al. 2009) in natural phytoplankton communities. However, this study has demonstrated the potential utility of this parameter for assessing the physiological status of natural *Emiliania huxleyi* populations when they are the dominant chl *a*-containing organisms in the microbial community. Although measurements of chl *a* fluorescence give information only about the state of PSII, electron transport rate through PSII is indicative, under many conditions, of the overall rate of photosynthesis (Maxwell & Johnson 2000). By assessing the changes in PSII photochemistry during infection and lysis in more detail, with simultaneous measurements of gas exchange and host biochemical composition, it may be possible to identify photophysiological markers for particular phases of viral-induced bloom termina-

tion. The consequences of viral-induced disruption of host PSII photochemistry pre-lysis may have important implications for oceanic primary production and the ecology and biogeochemical cycling of marine food webs, particularly in globally significant species like *E. huxleyi*. Therefore, developing a detailed, mechanistic understanding of the viral-driven changes in *E. huxleyi* PSII photochemical activity during infection, using controlled laboratory physiological manipulations, is crucial and should be a future direction for research.

**Acknowledgements.** This research was supported by a grant awarded to W.H.W. from the Natural Environment Research Council (NERC) (ref NE/D001455/1). The study also formed part of the NERC Oceans 2025 programme through which S.A.K. and M.J.A. were funded at PML. W.H.W. was supported by a National Science Foundation (NSF) grant ref. EF0723730. We thank C.R. Budinoff for providing chlorophyll data. The authors also thank all the participants of the mesocosm, the staff of Espeland Station and the University of Bergen for making our stay both highly enjoyable and productive. Thanks also to S.D. Archer for his insightful comments and suggestions that improved this manuscript, and 3 anonymous reviewers for their constructive and helpful remarks.

#### LITERATURE CITED

- Asada K (1994) Production and action of active oxygen species in photosynthetic tissues. In: Foyer CH, Mullineaux PM (eds) Causes of photooxidative stress and amelioration of defence systems in plants. CRC Press, Boca Raton, FL, p 77–104
- Baker NR (2008) Chlorophyll fluorescence: a probe of photosynthesis in vivo. *Annu Rev Plant Biol* 59:89–113
- Balachandran S, Hurry VM, Kelley SE, Osmond CB and others (1997) Concepts of plant biotic stress. Some insights into the stress physiology of virus-infected plants, from the perspective of photosynthesis. *Physiol Plant* 100:203–213
- Behrenfeld MJ, Prasil O, Kolber ZS, Babin M, Falkowski PG (1998) Compensatory changes in photosystem II electron turnover rates protect photosynthesis from photoinhibition. *Photosynthesis Res* 58:259–268
- Bidle KD, Vardi A (2011) A chemical arms race at sea mediates algal host–virus interactions. *Curr Opin Microbiol* 14:449–457
- Bidle KD, Haramaty L, Barcelos e Ramos J, Falkowski P (2007) Viral activation and recruitment of metacaspases in the unicellular coccolithophore, *Emiliana huxleyi*. *Proc Natl Acad Sci USA* 104:6049–6054
- Bratbak G, Egge JK, Heldal M (1993) Viral mortality of the marine alga *Emiliana huxleyi* (Haptophyceae) and termination of algal blooms. *Mar Ecol Prog Ser* 93:39–48
- Brown CM, Campbell DA, Lawrence JE (2007) Resource dynamics during infection of *Micromonas pusilla* by virus MpV-Sp1. *Environ Microbiol* 9:2720–2727
- Brussaard CPD (2004) Optimization of procedures for counting viruses by flow cytometry. *Appl Environ Microbiol* 70:1506–1513
- Burkill PH, Archer SD, Robinson C, Nightingale PD, Groom SB, Tarran GA, Zubkov MV (2002) Dimethyl sulphide biogeochemistry within a coccolithophore bloom (DISCO): an overview. *Deep-Sea Res II* 49:2863–2885
- Castberg T, Larsen A, Sandaa RA, Brussaard CPD and others (2001) Microbial population dynamics and diversity during a bloom of the marine coccolithophorid *Emiliana huxleyi* (Haptophyta). *Mar Ecol Prog Ser* 221:39–46
- Cullen JJ, Davis RF (2003) The blank can make a big difference in oceanographic measurements. *Limnol Oceanogr Bull* 12:29–35
- Cullen JJ, Yang X, MacIntyre HL (1992) Nutrient limitation of marine photosynthesis. In: Falkowski PG, Woodhead AD (eds) Primary productivity and biogeochemical cycles in the sea. Plenum Press, New York, NY, p 31–45
- Egge JK, Aksnes DL (1992) Silicate as regulating nutrient in phytoplankton competition. *Mar Ecol Prog Ser* 83: 281–289
- Egge JK, Heimdal BR (1994) Blooms of phytoplankton including *Emiliana huxleyi* (Haptophyta). Effects of nutrient supply in different N:P ratios. *Sarsia* 79:333–348
- Evans C, Malin G, Mills GP, Wilson WH (2006) Viral infection of *Emiliana huxleyi* (Prymnesiophyceae) leads to elevated production of reactive oxygen species. *J Phycol* 42:1040–1047
- Falkowski PG, Raven JA (2007) Aquatic photosynthesis, Princeton University Press, Princeton, NJ
- Frada M, Probert I, Allen MJ, Wilson WH, de Vargas C (2008) The ‘Cheshire cat’ escape strategy of the coccolithophore *Emiliana huxleyi* in response to viral infection. *Proc Natl Acad Sci USA* 105:15944–15949
- Fritz JJ, Balch WM (1996) A light-limited continuous culture study of *Emiliana huxleyi*: determination of coccolith detachment and its relevance to cell sinking. *J Exp Mar Biol Ecol* 207:127–147
- Gachon CMM, Küpper H, Küpper FC, Stik I (2006) Single-cell chlorophyll fluorescence kinetic microscopy of *Pyraliella littoralis* (Phaeophyceae) infected by *Chytridium polysiphoniae* (Chytridiomycota). *Eur J Phycol* 41: 395–403
- Geider RJ, La Roche J (1994) The role of iron in phytoplankton photosynthesis, and the potential for iron-limitation of primary productivity in the sea. *Photosynth Res* 39: 275–301
- Geider R, La Roche J (2002) Redfield revisited: variability of C: N: P in marine microalgae and its biochemical basis. *Eur J Phycol* 37:1–17
- Geider RJ, LaRoche J, Greene RM, Olaizola M (1993) Response of the photosynthetic apparatus of *Phaeodactylum tricorutum* (Baccillariophyceae) to nitrate, phosphate or iron starvation. *J Phycol* 29:755–766
- Graziano LM, Geider RJ, Li WKW, Olaizola M (1996) Nitrogen limitation of North Atlantic phytoplankton: analysis of physiological condition in nutrient enrichment experiments. *Aquat Microb Ecol* 11:53–64
- Hewson I, O’Neil JM, Dennison WC (2001) Virus-like particles associated with *Lyngbya majuscula* (Cyanophyta; Oscillatoriaceae) bloom decline in Moreton Bay, Australia. *Aquat Microb Ecol* 25:207–213
- Jacquet S, Heldal M, Iglesias-Rodriguez D, Larsen A, Wilson W, Bratbak G (2002) Flow cytometric analysis of an *Emiliana huxleyi* bloom terminated by viral infection. *Aquat Microb Ecol* 27:111–124
- Juneau P, Lawrence JE, Suttle CA, Harrison PJ (2003)

- Effects of viral infection on photosynthetic processes in the bloom-forming alga *Heterosigma akashiwo*. *Aquat Microb Ecol* 31:9–17
- Klausmeier CA, Litchman E, Daufresne T, Levin SA (2004) Optimal nitrogen-to-phosphorus stoichiometry of phytoplankton. *Nature* 429:171–174
- Kolber Z, Falkowski PG (1993) Use of active fluorescence to estimate phytoplankton photosynthesis in-situ. *Limnol Oceanogr* 38:1646–1665
- Kolber Z, Zehr J, Falkowski P (1988) Effects of growth irradiance and nitrogen limitation on photosynthetic energy conversion in photosystem II. *Plant Physiol* 88:923–929
- Kolber ZS, Prášil O, Falkowski PG (1998) Measurements of variable chlorophyll fluorescence using fast repetition rate techniques: defining methodology and experimental protocols. *Biochim Biophys Acta* 1367.1:88–106
- Kruskopf M, Flynn KJ (2006) Chlorophyll content and fluorescence responses cannot be used to gauge reliably phytoplankton biomass, nutrient status or growth rate. *New Phytol* 169:525–536
- Lessard EJ, Merico A, Tyrrell T (2005) Nitrate: phosphate ratios and *Emiliana huxleyi* blooms. *Limnol Oceanogr* 50:1020–1024
- Lindell D, Jaffe JD, Johnson ZI, Church GM, Chisholm SW (2005) Photosynthesis genes in marine viruses yield proteins during host infection. *Nature* 438:86–89
- Llewellyn CA, Evans C, Ains RL, Cook I, Bale N, Wilson WH (2007) The response of carotenoids and chlorophylls during virus infection of *Emiliana huxleyi* (Prymnesiophyceae). *J Exp Mar Biol Ecol* 344:101–112
- Marie D, Brussaard CPD, Thyrhaug R, Bratbak G, Vaulot D (1999) Enumeration of marine viruses in culture and natural samples by flow cytometry. *Appl Environ Microbiol* 65:45–52
- Martínez Martínez J, Schroeder DC, Larsen A, Bratbak G, Wilson WH (2007) Molecular dynamics of *Emiliana huxleyi* and co-occurring viruses during 2 separate mesocosm studies. *Appl Environ Microbiol* 73:554–562
- Martínez Martínez JM, Poulton NJ, Stepanauskas R, Sieracki ME, Wilson WH (2011) Targeted sorting of single virus-infected cells of the coccolithophore *Emiliana huxleyi*. *PLoS One* 6:e22520
- Maxwell K, Johnson GN (2000) Chlorophyll fluorescence—a practical guide. *J Exp Bot* 51:659–668
- Moore CM, Suggett DJ, Hickman AE, Young-Nam K and others (2006) Phytoplankton photoacclimation and photoadaptation in response to environmental gradients in a shelf sea. *Limnol Oceanogr* 51:936–949
- Moore CM, Mills MM, Langlois R, Milne A, Achterberg EP, La Roche J, Geider RJ (2008) Relative influence of nitrogen and phosphorus availability on phytoplankton physiology and productivity in the oligotrophic sub-tropical North Atlantic Ocean. *Limnol Oceanogr* 53:291–305
- Morel A, Ahn YH, Partensky F, Vaulot D, Claustre H (1993) *Prochlorococcus* and *Synechococcus*: a comparative study of their optical properties in relation to their size and pigmentation. *J Mar Res* 51:617–649
- Muggli DL, Harrison PJ (1996) Effects of nitrogen source on the physiology and metal nutrition of *Emiliana huxleyi* grown under different iron and light conditions. *Mar Ecol Prog Ser* 130:255–267
- Paasche E (2002) A review of the coccolithophorid *Emiliana huxleyi* (Prymnesiophyceae), with particular reference to growth, coccolith formation, and calcification-photosynthesis interactions. *Phycologia* 40:503–529
- Pagarete A, Allen MJ, Wilson W, Kimmance SA, de Vargas C (2009) Host-virus shift of the sphingolipid pathway along an *Emiliana huxleyi* bloom: survival of the fittest. *Environ Microbiol* 11:2840–2848
- Parkhill JP, Maillet G, Cullen JJ (2001) Fluorescence-based maximal quantum yield for PSII as a diagnostic of nutrient stress. *J Phycol* 37:517–529
- Parsons TR, Maita Y, Lalli CM (1984) A manual of chemical and biological methods for seawater analysis. Pergamon Press, Oxford
- Pond DW, Harris RP (1996) The lipid composition of the coccolithophore *Emiliana huxleyi* and its possible eco-physiological significance. *J Mar Biol Assoc UK* 76: 579–594
- Ragni M, Ains R, Leonardos N, Archer S, Geider RJ (2008) Photoinhibition of PSII in *Emiliana huxleyi* (Haptophyta) under high light stress: the roles of photoacclimation, photoprotection and photorepair. *J Phycol* 44:670–683
- Rahoutei J, García-Luque I, Barón M (2000) Inhibition of photosynthesis by viral infection: effect on PSII structure and function. *Physiol Plant* 110:286–292
- Schroeder DC, Oke J, Hall M, Malin G, Wilson WH (2003) Virus succession observed during an *Emiliana huxleyi* bloom. *Appl Environ Microbiol* 69:2484–2490
- Schwarz KB (1996) Oxidative stress during viral infection: a review. *Free Radic Biol Med* 21:641–649
- Seaton G, Lee K, Rohozinski J (1995) Photosynthetic shutdown in *Chlorella* NC64A associated with infection cycle of *Paramecium-Bursaria Chlorella virus-1*. *Plant Physiol* 108:1431–1438
- Seaton GG, Hurry VM, Rohozinski J (1996) Novel amplification of non-photochemical chlorophyll fluorescence quenching following viral infection in *Chlorella*. *FEBS Lett* 389:319–323
- Smyth TJ, Pemberton KL, Aiken J, Geider RJ (2004) A methodology to determine primary production and phytoplankton photosynthetic parameters from Fast Repetition Rate Fluorometry. *J Plankton Res* 26:1337–1350
- Sorensen G, Baker A, Hall MJ, Munn CB, Schroeder DC (2009) Novel virus dynamics in an *Emiliana huxleyi* bloom. *J Plankton Res* 31:787–791
- Strickland JDH, Parsons TR (1968) A practical handbook of seawater analysis. *Bull Fish Res Board Can* 167: 1–34
- Suggett DJ, MacIntyre HL, Geider RJ (2004) Evaluation of biophysical and optical determinations of light absorption by photosystem II in phytoplankton. *Limnol Oceanogr Meth* 2:316–332
- Suggett DJ, Moore CM, Hickman AE, Geider RJ (2009) Interpretation of fast repetition rate (FRR) fluorescence: signatures of phytoplankton community structure versus physiological state. *Mar Ecol Prog Ser* 376:1–19
- Suttle CA (1992) Inhibition of photosynthesis in phytoplankton by the submicron size fraction concentrated from seawater. *Mar Ecol Prog Ser* 87:105–112
- Suttle CA (2007) Marine viruses - major players in the global ecosystem. *Nat Rev Microbiol* 5:801–812
- Suttle CA, Chan AM (1993) Marine cyanophages infecting oceanic and coastal strains of *Synechococcus*: abundance, morphology, cross-infectivity and growth characteristics. *Mar Ecol Prog Ser* 92:99–109
- Suttle CA, Chan AM, Cottrell MT (1990) Infection of phytoplankton by viruses and reduction of primary productivity. *Nature* 347:467–469
- Sylvan JB, Quigg A, Tozzi S, Ammerman JW (2007) Eutrophication-induced phosphorus limitation in the Missis-

- issippi River plume: Evidence from fast repetition rate fluorometry. *Limnol Oceanogr* 52:2679–2685
- Teklemariam TA, Demeter S, Deák Z, Surányi G, Borbély G (1990) AS-1 cyanophage infection inhibits the photosynthetic electron flow of photosystem II in *Synechococcus* sp. PCC 6301, a cyanobacterium. *FEBS Lett* 270:211–215
- Thingstad TF, Lignell R (1997) Theoretical models for the control of bacterial growth rate, abundance, diversity and carbon demand. *Aquat Microb Ecol* 13:19–27
- Timmermans KR, Gerringa LJA, de Baar HJW, van der Wagt B, Veldhuis MJW, de Jong JTM, Croot PL (2001) Growth rates of large and small Southern Ocean diatoms in relation to availability of iron in natural seawater. *Limnol Oceanogr* 46:260–266
- Van Etten JL, Burbank DE, Xia Y, Meints RH (1983) Growth cycle of a virus, PBCV-1, that infects *Chlorella*-like algae. *Virology* 126:117–125
- Van Etten JL, Lane LC, Meints RH (1991) Viruses and virus-like particles of eukaryotic algae. *Microbiol Rev* 55: 586–620
- Vardi A, Van Mooy BAS, Fredricks HF, Popenorf KJ, Ossolinski JE, Haramaty L, Bidle KD (2009) Viral glycosphingolipids induce lytic infection and cell death in marine phytoplankton. *Science* 326:861–865
- Vardi A, Haramaty L, Van Mooy BA, Fredricks HF, Kimman SA, Larsen A, Bidle KD (2012) Host–virus dynamics and subcellular controls of cell fate in a natural coccolithophore population. *Proc Natl Acad Sci* 109: 19327–19332
- Vassiliev IR, Prasil O, Wyman KD, Kolber ZS, Hanson KA, Prentice JE, Falkowski PG (1994) Inhibition of PSII photochemistry by PAR and UV radiation in natural phytoplankton communities. *Photosynth Res* 42:51–64
- Volk T, Hoffert MI (1985) The carbon cycle and atmospheric CO<sub>2</sub>: natural variations Archean to present. *Geophys Monogr Ser* 32:99–111
- Waters RE, Chan AT (1982) *Micromonas pusilla* virus: the virus growth cycle and associated physiological events within the host cells; host range mutation. *Virology* 63: 199–206
- Westbroek P, Brown CW, van Bleijswijk J, Brownlee C and others (1993) A model system approach to biological climate forcing. The example of *Emiliana huxleyi*. *Global Planet Change* 8:27–46
- Wilhelm SW, Suttle CA (1999) Viruses and nutrient cycles in the sea. *Bioscience* 49:781–788
- Wilson WH, Tarran GA, Schroeder D, Cox M, Oke J, Malin G (2002) Isolation of viruses responsible for the demise of an *Emiliana huxleyi* bloom in the English Channel. *J Mar Biol Assoc UK* 82:369–377
- Wolfe GV, Steinke M (1996) Grazing-activated production of dimethyl sulfide (DMS) by 2 clones of *Emiliana huxleyi*. *Limnol Oceanogr* 41:1151–1160
- Young E, Beardall J (2003) Transient perturbations in chlorophyll a fluorescence elicited by nitrogen re-supply to nitrogen-stressed microalgae: distinct responses to NO<sub>3</sub><sup>-</sup> versus NH<sub>4</sub><sup>+</sup>. *J Phycol* 39:332–342
- Zubkov MV, Tarran GA (2008) High bacterivory by the smallest phytoplankton in the temperate North Atlantic Ocean. *Nature* 455:224–226

*Editorial responsibility: Katherine Richardson, Copenhagen, Denmark*

*Submitted: May 17, 2013; Accepted: August 18, 2013  
Proofs received from author(s): December 3, 2013*